Corrosion and Corrosion Product Transport in Lithium-Cooled Stainless Steel Fusion Reactor Circuits

A.B. Johnson, Jr. and W.F. Vogelsang

July 1973

UWFDM-54

FUSION TECHNOLOGY INSTITUTE

UNIVERSITY OF WISCONSIN

MADISON WISCONSIN

Corrosion and Corrosion Product Transport in Lithium-Cooled Stainless Steel Fusion Reactor Circuits

A.B. Johnson, Jr. and W.F. Vogelsang

Fusion Technology Institute
University of Wisconsin
1500 Engineering Drive
Madison, WI 53706

http://fti.neep.wisc.edu

July 1973

UWFDM-54

CORROSION AND CORROSION PRODUCT TRANSPORT IN LITHIUM-COOLED STAINLESS STEEL FUSION REACTOR CIRCUITS

by

A. B. Johnson, Jr.

and

W. F. Vogelsang

July 1973

FDM 54

Introduction

The University of Wisconsin Toroidal Fusion Reactor (UWMAK-1) comprises the following major systems where corrosion potential exists (refer to Figure 1):

- the lithium-cooled primary circuit including the first wall, lithium blanket, headers and the intermediate heat exchanger (lithium-to-lithium);
- the secondary lithium circuit, including two heat exchangers and associated headers;
- the steam system, including the lithium-to-steam heat exchanger, turbine, condenser, preheater and associated headers;
- the tritium extraction system, consisting principally of a tritium getter (yttrium metal) and associated tanks and piping;
- the lithium cleanup systems, which will consist principally of a hot trap (zirconium getter bed) and a cold trap, (stainless steel mesh) and associated tanks and piping;
- the helium system for cooling the shield (not shown in Figure 1).

The design material in the liquid metal circuits is 316 stainless steel (see Table I for metal composition). The lithium-to-lithium heat exchanger design material is 304L SS, on the evidence that tritium permeation rates are mildly lower for 304 than 316 SS.[1] Evidence of relatively poor corrosion resistance of nickel-base alloys in lithium leaves some doubt regarding the optimum material for the

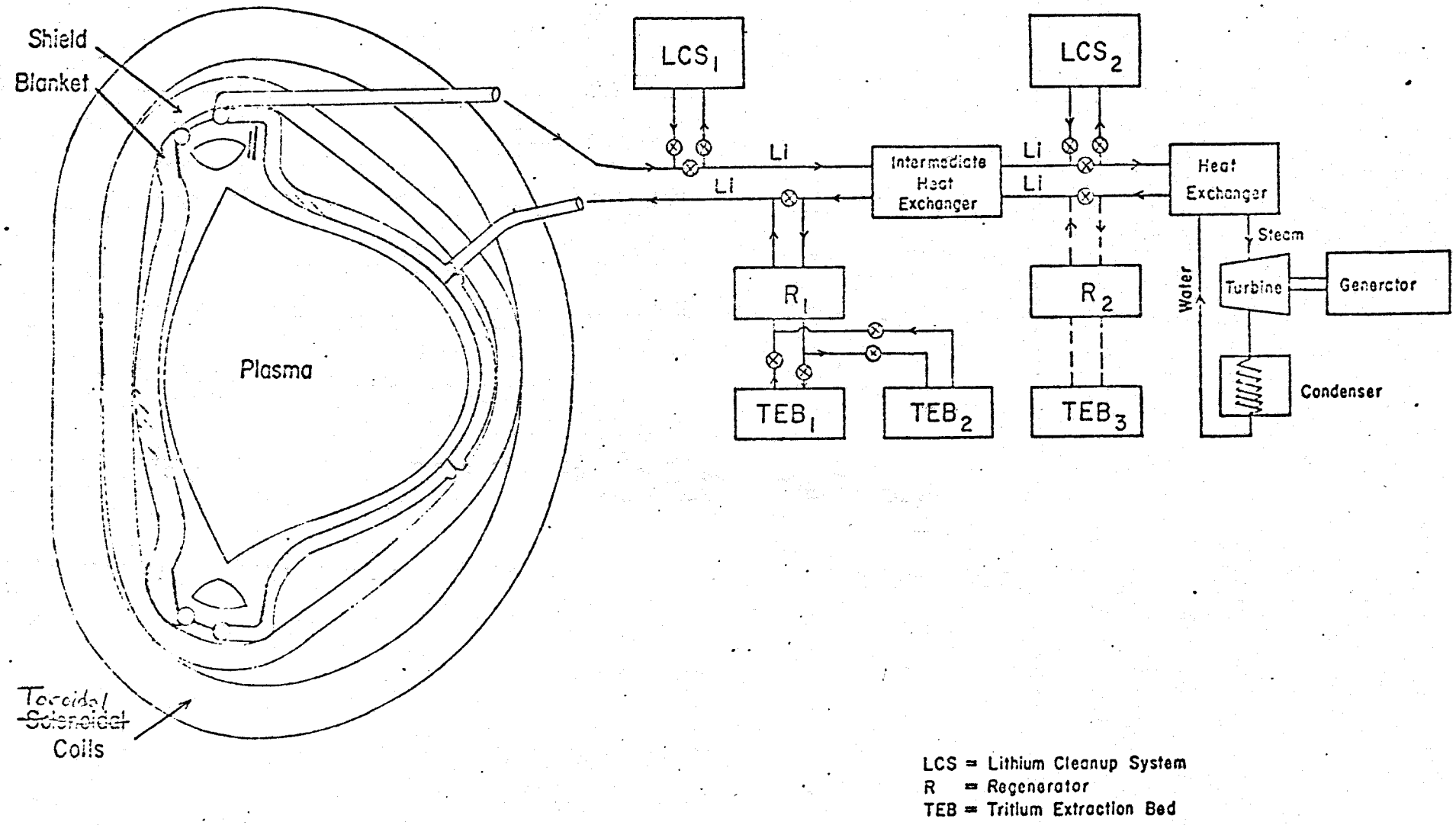

FIG. 1 Schematic Plant Design — UW. Toroidal Fusion Reactor

Table I

Stainless Steel Composition Specifications

316 Stainless Steel Weight Percent	Element	304L Stainless Steel Weight Percent
	Fe	
16/18	Cr	18/20
10/14	Ni	8/12
2.0/3.0	Mo	-
2.0 max.	Mn	2.0 max.
1.0 max	Si	1.0 max.
0.080 max.	C	0.030 max.
0.045 max.	P	0.045 max.
0.030 max.	S	0.030 max.

lithium-to-steam heat exchanger. Incoloy 800 was the material selected for an Na-to-H_2) heat exchanger in a sodium-cooled system.[2] However, due to the uncertainty regarding Incoloy corrosion behavior in lithium and the likelihood of somewhat higher tritium diffusion rates in Incoloy, the design material for the Li-to-H_2O heat exchanger is 304L SS.

The subjects addressed in this treatment will be: lithium-stainless steel compatibility; corrosion product transport; corrosion in auxiliary systems; and lithium purity. The corrosion of stainless steel will be compared to corrosion behavior of other candidate Controlled Thermonuclear Reactor (CTR) materials. The principal alternate materials now being considered are molybdenum, niobium, vanadium and their alloys. Stainless steel behavior in lithium and in flibe (lithium beryllium fluoride) also will be compared.

Lithium - Stainless Steel Compatibility

The size parameters and exposure conditions in the primary and secondary lithium circuits and the steam system are summarized in Table II.

Lithium Corrosion

Early corrosion results[3] indicated that iron, niobium, tantalum and molybdenum had good corrosion resistance to lithium up to 900°C; ferritic steels were resistant to lithium to ~800°C; austenitic steels had good resistance to ~500°C; nickel and its alloys had only limited resistance at 300-500°C. However, the studies often were conducted in lithium of questionable purity, precluding full confidence in the results.

There are essentially no long-term corrosion parameter studies for stainless steel in lithium. Projections of corrosion behavior therefore must be based on short-term data. Systematic studies of impurity effects also are largely lacking.[4]

Gill, et al performed a series of corrosion tests in lithium over a temperature range from 510 to 612°C.[5] The tests were conducted principally on 304 SS, but corrosion on other 300-series steels did not differ statistically from results on 304 SS. Corrosion rates from the study are summarized in Table III as a function of temperature.

The data in Table III were determined for lithium flow rates in the range of 15 to 85 cm/sec, which are low compared to typical dynamic liquid metal systems. However, the magneto-hydrodynamic (MHD) effect[6] in lithium flowing in intense magnetic fields preclude high flow rates. The maximum design flow rate in the blanket is 5 cm/sec;

Table II

U. W. Toroidal Fusion Reactor Parameters

Plant Rating	5000 MW_{th}
Major Radius	13 m
Minor Radius	5.5 m
Primary Lithium Circuit	
Area in Contact with Lithium	$6 \times 10^4 m^2$
Lithium Weight	$8 \times 10^5 kg$
Lithium Inlet Temperature	283°C
Lithium Outlet Temperature	483°C
Lithium Linear Flow Rate (Blanket)	5.0 cm/sec
Lithium Linear Flow Rate (Headers)	125 cm/sec
Lithium Mass Flow Rate	$2.1 \times 10^7 kg/hr$
Intermediate Heat Exchanger Area	$1.1 \times 10^4 m^2$
Neutron Flux, E = 0 - 14 Mev (Lithium-side of first wall)	$4.7 \times 10^{14} n/cm^2 sec$ [a]
Secondary Lithium Circuit	
Area in Contact with Lithium	$3.9 \times 10^4 m^2$
Lithium Weight	$10^5 kg$
Lithium Inlet Temperature	235°C
Lithium Outlet Temperature	445°C
Lithium Mass Flow Rate	$2 \times 10^7 kg/hr$
Steam/Water Circuit	
Heat Exchanger Area	$2.8 \times 10^4 m^2$
Maximum Steam Temperature	425°C
Maximum Steam Pressure	600 psi
Steam Flow Rate	7×10^5 kg/hr.

a. The primary current of 14 Mev neutrons is $5.7 \times 10^{13} n/cm^2 sec$

Table III

Corrosion Rates for Stainless Steel in Lithium[5]

Temperature °C	Corrosion Rate[a.] mg/cm^2 mo	um/y
300 (extrapolated)	0.01	0.15
400	0.11	1.6
500	1	15
550	3	45
600	6	90

a. Penetration of 25 um into a stainless steel surface corresponds to a weight loss of ~20 mg/cm^2.

at locations in the primary circuit where MHD effects are small, anticipated flow rates are up to 125 cm/sec. The data of Gill, et al suggest that corrosion rates were not strongly influenced by lithium flow rates in the range of their tests. Corrosion rates for a 1Cr18Ni9Ti steel in lithium at 700-900°C were higher under natural convection than in static lithium, but the effect was not large.[4] It will be assumed that the data in Table III account for flow rate effects on corrosion in the UWMAK-1, until fully pertinent data are available.

At the UWMAK-1 inlet and outlet temperature extremes (~300 and 500°C) the corresponding thermal corrosion rates are 0.15 and 15 um/y. These corrosion rates can be accomodated in the design thickness of the primary

and secondary system components. Maximum metal penetration from thermal corrosion will be 0.03 mm for the anticipated 2-year first wall life and 0.3 m for the 20-year design life of other components. Potential contributions to the corrosion rate from radiation effects will be discussed in the following section. It would be desirable on thermal efficiency grounds to increase the lithium temperature. Estimates of the limiting temperature for stainless steel-lithium compatibility vary: Ref. 3 indicates 500°C; Ref. 5 suggests ~590°C. In another study, iron and austenitic stainless steels underwent severe solution corrosion, intergranular attack and mass transfer at 700 to 815°C. Type 316 SS was said to be suitable for only limited service at 590°C in a loop having a 100°C termperature gradient.(7) While penetration rates in Table III at 600°C may be acceptable from a structural standpoint, they magnify an already-serious corrosion transport problem, treated in a later section. Thus, if the corrosion rates indicated in Table III accurately represent corrosion product transport rates in the UWMAK-1, further increases in temperature appear undesirable.

The release of corrosion products from stainless steel does not generally occur in the stoichiometry shown in Table I for alloy constitutents. Nickel was leached preferentially from 304 SS exposed to high-purity lithium at 500-600°C.(5) Deposits in the low-temperature loop region were high in nickel; Cr, Mn, Si and C also were detectable. In another study, nickel was removed preferentially from 316 SS in lithium at 590-769°C.(8) The attack was largely transgranular. Gamma iron

was found in cold-zone deposits. At 760-870°C, the attack was intergranular; when sigma phase was present, the cold-zone deposit was high in Cr, Ni and Fe. When sigma phase was absent, the cold-zone deposit was high in Ni and low in Cr. Carbon transport occurred when sigma phase was absent in low-nitrogen lithium. The carbon deposited in the cold zone as iron carbides. Tests in lithium above 540°C resulted in selective attack on nickel and carbon in austentic stainless steels.[3]

Selective leaching also occurs in refractory metal systems. A Nb-1Zr alloy exposed to lithium at 1200°C (150°C ΔT) lost nitrogen, carbon and zirconium, which deposited in the cold region, principally as zirconium nitride.[9] Chromium depletion was a predominant effect in stainless steel surfaces exposed to flibe at a maximum temperature of 688°C.[10]

A few studies are reported indicating effects of contaminants on stainless steel corrosion in lithium. High-purity lithium contaminated with 0.36 percent air reacted rapidly with 304 SS at 816°C, resulting in tube plugging after 72 hours.[11] Chromium was selectively removed from the stainless steel to depths of 10 mm under these conditions. In high-purity lithium, only mild intergranular attack occurred after 720 hours at 816°C. Chromium appeared to have an unusually high solubility in lithium in these studies, compared to data shown in Figure 2; selective leaching of nickel was not observed, in contrast to studies cited earlier.[3,5,8] Furthermore, the corrosion rates in high-purity lithium appeared to be surprisingly low.

In Russian work cited earlier, corrosion rates were measured on a 1Cr18Ni9Ti steel in lithium at 700, 800 and 900°C. Weight losses corresponded to a metal penetration of ~30 um in 1000 hours at 700°C in static, contaminated lithium (~19% O_2 and 1% H_2 by weight); penetrations in high-purity static lithium were 8-15 um in 1000 hours. One weight percent nitrogen caused substantial increases in corrosion rate, while a similar oxygen concentration had little effect. Corrosion rates in static lithium were initially rapid, but decreased with time, apparently as the solution became saturated with corrosion products. Lithium flowing by natural convection caused corrosion rates higher than those in static lithium, due to mass transport effects. In the flowing system, specimens lost weight in the hot zone and corrosion products were transferred to the cold zone. The attack was largely intergranular. There was considerable evidence of selective nickel transport between materials with differing nickel contents.

Hoffman reported that nitrogen contamination in lithium resulted in accelerated corrosion of 316 SS at 870°C.[12] Devries reported that stainless steels, (including 316 SS) had good corrosion and stress corrosion resistance in air-contaminated lithium at 315 and 480°C, but the tests were short (up to seven days).[13]

Oxygen has a significant effect on stainless steel corrosion in sodium, and there are indications that it may be desirable to operate Liquid Metal Fast Breeder (LMFBR) systems at <2 ppm oxygen.[14] The emerging evidence for lithium suggests that nitrogen may be more significant than oxygen in stainless steel corrosion.

The corrosion of niobium and tantalum in static lithium was not affected by oxygen concentrations of 100-2000 ppm in the lithium, contrary to behavior in sodium.[15] On the other hand, oxygen dissolved in the refractory metals, above some threshold value (~400 ppm for Nb), caused rapid intergranular penetration by lithium. Zirconium alloy additions serve to getter the oxygen in the Nb and Ta and preclude the rapid penetration by lithium. Russian work indicates that oxygen dissolved in steel also enhances lithium penetration.[4a]

Fusion reactors constructed from the refractory metals are projected to operate at substantially higher temperatures than the 500°C maximum UWMAK-1 design temperature. Even at temperatures above 800°C, corrosion rates for the refractory metals generally are reported as "nil" or "slight". Selected exposures of refractory metals to lithium are summarized below:

Material	Max. Temp °C	Thermal Gradient, °C	Velocity m/sec	Test Time hr.
Vanadium[16]	870	204	4.0	1194
Mo-0.5Ti[16]	815	93	4.0	694
Nb-1Zr[9]	1200	100-150	3.2	3000

Corrosion and mass transfer rates for V and Mo-0.5Ti were reported as nil after the above exposures. The weight loss from Nb-1Zr was up to 0.3 mg/cm^2 (0.07 mg/cm^2 Mo), which is similar to the stainless steel mass transfer rate at ~375°C (Table III).

Corrosion data for stainless steels in a molten salt ($LiF-BeF_2-ThF_4-UF_4$) indicate a maximum corrosion rate of 50 um/y at a hot leg

temperature of 688°C and a cold leg temperature of 588°C.[10] Grain boundary attack and voids extended into the matrix apparently due to selective chromium diffusion from the specimen. Weight losses occurred over exposures up to 32,000 hr.; the corrosion rates decreased with decreasing temperature over the range of 688 to 668°C. The corrosion rate was controlled by the solid state diffusion of chromium.

Another molten salt test series at 663°C indicated a corrosion rate of 28 um/y for 304 SS. At 650°C, 316 SS corroded at maximum rates 20-25 um/y. However, only a fraction of the system area corroded at the maximum rates.

Irradiation Effects on Corrosion

Irradiation of Type 316 stainless steel in lithium was reported to have no effect on corrosion at 540°C,[17] but the neutron fluences ($3\text{-}7 \times 10^{16}$ n/cm^2) were too low to draw definitive conclusions. Limited evidence suggests that radiation does not accelerate corrosion rates of stainless steel in sodium.[18] However, there is speculation that in high-flux sodium-cooled reactors, fast neutron sputtering would add substantially to corrosion rates[19], involving damage to rate-limiting ferrite layer. Similar layers also are reported to form on stainless steel exposed to lithium[5,8] and to flibe.[10] Whether such a layer would in fact develop on stainless steel at 500°C is not clear, but it would almost certainly be very thin (probably $<<1$ um).

Sputtering rates for stainless steel were calculated by Anno and Walowit to be 38 um/y at a fast neutron flux of 10^{16} n/cm^{2}sec, applying

a sputtering ratio for Cu(2×10^{-3}) in the absence of direct data for stainless steel.[19] At 600-700°C in sodium, the ferrite layer on stainless steel reaches a steady state thickness of ~10 um.[20] Assuming that the ferrite layer thickness controls the corrosion rate, the sputtering rate indicated above would have two effects on material transport: a) direct removal of material from the ferrite layer; b) thinning of the layer, resulting in increased corrosion of the steel substrate.

The calculated neutron current for the UWMAK-1 is 5.7×10^{13} 14 MeV neutrons per square centimeter on the first wall. The neutron flux on the inside surface of the first wall is 4.7×10^{14} n/cm^2, E, 0 to 14 MeV; greater than 99 percent of the neutrons have energies above 0.1 MeV. Using an estimated sputtering ratio for iron of 9×10^{-3} atoms/n[21], the sputtering loss from the inside surface of the first wall is estimated to be 16 um/y, based on the relationship:

$$\text{Metal Loss} = \frac{S\ \phi t\ A}{No\ \rho}$$

where, S is sputtering ratio (atoms/neutron); ϕt is neutron fluence; A is atomic weight; No is atom number density; ρ is metal density. Any ferrite or other solid state diffusion zone which develops on stainless steel in lithium at 500°C almost certainly will be this ($<<1$ um). Therefore, the above calculation suggests that sputtering may be a rate - controlling factor on the corrosion of the first wall inner surface. The area of the first wall surface is ~4×10^3 m^2, slightly less than 10 percent of the total primary circuit area. Neutron attenuation probably will preclude major sputtering problems in other

regions of the circuit. From the above calculation, sputtering would increase the corrosion product inventory in the primary circuit by ~10 percent (250 kg/y) by direct removal, but may have an additional accelerating effect if the corrosion rate is in fact controlled by solid state diffusion through the surface layer which is sputtered away. The effect of sputtering on corrosion appears to offer a potential accelerating effect on corrosion which appears to justify experimental study.

It also is possible that other radiation effects may accelerate corrosion processes in the lithium system. While direct parallels between aqueous and liquid metal systems are not justified, unusual effects of radiation on corrosion have occurred in aqueous systems which were not anticipated from experiments in unirradiated systems.[22] No unusual radiation effects have been recognized for stainless steel corrosion in sodium, but much less is known about the corrosion behavior of stainless steel or refractory metals in lithium.

Solubilities of Selected Elements in Lithium

While liquid-phase solubility is not necessarily rate-determining in liquid metal corrosion, it is an important consideration in evaluating corrosion and corrosion product transport mechanisms. Solubilities of stainless steel constitutents[23] and refractory metals[23,24] have been summarized. Solubility data from Ref. 23 are shown in Figure 2 indicating that the solubility of nickel in lithium is nearly two orders of magnitude higher than the solubilities of chromium and iron,

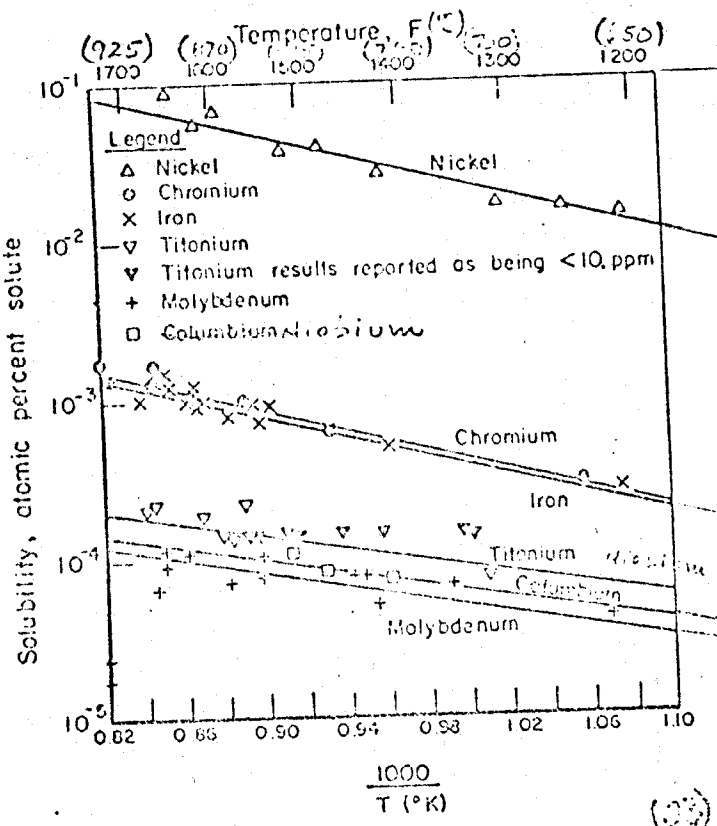

FIGURE 2. SOLUBILITY OF SOME METALS IN LITHIUM

Nitrogen contamination 25 to 150 ppm.

and nearly three orders of magnitude higher than the refractory metals. The summary of solubility data in Ref. 24 indicates considerable variation in results from one observer to another, suggesting that solubilities in lithium must be applied with caution on present knowledge.

The temperature range for the data in Figure 2 is above the design temperature range for the UWMAK-1. If the solubility trends continue at lower temperatures, the solubilities will be approximately as shown in Table IV.

When saturated at 500°C, the UWMAK-1 primary coolant (8×10^5 kg Li) would contain ~280 kg of Ni. The significance of corrosion product transport to plant operation will be discussed in a later section.

Table IV

Solubilities of Selected Elements in Lithium[a)]

Element	Solubility, ppm by wt.[b)]	
	500°C	300°C
Nickel	350	80
Iron, Chromium	8	2
Niobium, Molybdenum	3	1

a) Extrapolated from data in the temperature range ~940 - 650°C, Ref. 23.

b) In the UWMAK-1 primary circuit, one ppm by weight is equal to ~0.8 kg.

Solubilities of nitrogen and oxygen in lithium are summarized in Table V.

Table V

Solubilities of Nitrogen and Oxygen in Lithium

Element	Temperature, °C		
	500°C	400	250
Nitrogen, ppm	-	12,100	400
Oxygen, ppm	1700 ppm	650 ppm	90 ppm

a) Extrapolated from data in the range 250-400°C cited in Ref. 24.

Consistent with the data in Table V, oxygen concentrations in lithium can be reduced to <100 ppm by cold trapping; nitrogen is less susceptible to removal by cold trapping, due to its relatively high solubility in lithium, even near the lithium melting point (186°C).[24]

Corrosion Mechanisms

Liquid metal corrosion mechanisms potentially include the following types of attack:[3,25]

a) solution attack - relatively uniform dissolution of the metal by the liquid metal;

b) selective dissolution - leaching of one or more alloy constituents;

c) direct alloying - formation of surface films from reactions between the solid and the liquid metal;

d) intergranular penetration - often a variation of selective dissolution, where minor alloy constituents which concentrate in grain boundaries are selectively attacked. The attack often is accelerated by stress.

e) erosion corrosion - mechanical attack by turbulent coolant, suspended particles, or in extreme cases, cavitation.

f) fretting corrosion - corrosion which results from vibration between two adjacent components in contact.

g) stress corrosion crocking - failure of a metal by the combined action of corrosion and mechanical stress.

The emerging data from stainless steel exposures in sodium,[19,20] lithium,[5,8] and flibe[10] indicate that mechanism b is important in all three systems. Selective removal of nickel and/or chromium leaves an iron-rich layer (identified as ferrite in the liquid metal systems). Subsequent corrosion rates are considered by some observers to be controlled by solid state diffusion through the iron-rich layer.[5,8,10,19] However, other mechaniatic interpretations have been presented for steel corrosion in sodium systems.[26]

Mechanism d also is important in lithium metal[3,8,11] and molten salt[10] systems. Mechanism e probably will be relatively unimportant in CTR lithium primary circuits, due to low lithium linear velocities. Higher flow rates may occur in secondary circuits, where MHD effects are not restrictive, imposing a concomitant increase in the likelihood of erosion corrosion effects.

Evaluation of mechanism f is highly empirical and difficult to predict without a detailed knowledge of component design and local exposure to conditions. Mechanism g also is difficult to predict on the basis of very few systematic stress corrosion studies. Russian work indicated that steel corrosion rates in lithium were accelerated by stress.[4a] A case of stress cracking was reported for 310 SS exposed to lithium.[27]

Austenitic stainless steels resisted stress cracking in air-contaminated lithium at 315 and 480°C, but the exposures were short.[13] Di Stefano and Litman reported that no examples of stress corrosion has occurred for refractory metals exposed to alkali metals.[25] However, the present approach to defining stress corrosion cracking behavior is largely empirical. Stress corrosion studies clearly will be a necessary factor in a CTR development program.

Summary of Thermochemical Relationships for Carbides, Nitrides and Oxide

The thermochemistry of selected carbides, nitrides and oxides appears in Appendix A. Several generalizations from the literature and from Appendix A are summarized below.

- Group IVB Metals (Ti, Zr, Hf) form oxides, nitrides, and carbides which are more stable than the corresponding lithium compounds[a] and are more stable than corresponding compounds from Groups VB, VIB and VIIB of the periodic table.[24]
- Group VB metals (V, Nb, Ta) form oxides which are less stable than Li_2O, but their nitrides and carbides are more stable than the corresponding lithium compounds.[24]
- Niobium, tantalum and vanadium lost oxygen to lithium; titanium and zirconium gettered oxygen from lithium at 816°C.[25]

---

a) Values in Appendix A-III show Li_2O to be slightly more stable than ZrO_2 in the range of 25 to 625°C; however, zirconium has functioned successfully as a getter in lithium systems.

- Regarding the major stainless steel constituents, Fe and Ni compounds are less stable than the corresponding lithium compounds; Cr carbide is slightly more stable than Li carbide, but the lithium oxide and nitride are more stable than the chromium compounds.

- Yttrium carbide and oxide appear to be slightly more stable than corresponding lithium compounds in the range of 500-650°C.

Mechanical Property Effects

Lithium may degrade stainless steel mechanical properties by[a] corrosion penetration, or[b] by addition to or removal of elements in the steel matrix. Data in Table III suggest that corrosion penetration will be acceptable from a mechanical property standpoint for stainless steel exposed to lithium at 500°C. Carburization and decarburization and other material transport phenomena have occurred in stainless steel exposed to lithium, portending that under certain conditions changes in mechanical properties may occur. A detailed analysis of possible mechanical property changes is beyond the scope of this treatment, but data from stainless steel exposures to lithium and sodium will be discussed.

The ultimate tensile strength (UTS) of a 1Cr18Ni8Ti steel decreased by 14% and the ductility increased slightly on exposure to lithium at 700 and 800°C under natural convection.[4] The major changes occurred prior to 200 hours, but a small downward trend in UTS was present at test termination (1000 hours). Short-term

(up to 500 hours) tests of the Cr-Ni-Ti steel in static lithium resulted in very little difference in UTS and elongation between specimens exposed to lithium and controls exposed to argon at 500°C.[4a] In long-term exposures at 700°C, strength decreased with time, but there was little difference between behavior of specimens exposed to pure stable lithium and those exposed to argon. Addition of 1 wt.% of nitrogen or 1 wt.% of oxygen to the lithium had only minor effects on strength. Carbide precipitation occurred in controls and specimens exposed to lithium, causing reductions in ductility (not quantified).

Reductions in strength occurred for Cr-Ni-Ti steel specimens exposed to flowing lithium in a loop with a hot zone at 700°C and a cold zone at 400°C.[4a]

Stress rupture experiments with 310 SS tubes exposed to lithium at 549 to 871°C showed no effect of exposure on tensile strength.[27]

Stress rupture properties of non-stabilized 304 and 316 stainless steels were degraded by sodium exposures for 10,000 hours at 705°C.[28] However, no changes in properties occurred in exposures at 620°C. Reduced strength at 705°C was due to loss of carbon and boron from the steels and concurrent sigma phase formation. Stabilized alloys (321, 347, Inconel-800) did not lose carbon but did lose boron and nitrogen, though in smaller quantities than non-stabilized alloys.

The above data suggest that high-purity lithium at 300-500°C probably will not induce performance-limiting degradation of stainless steel mechanical properties, provided that the presence of zirconium hot traps and tritium getter materials do not cause excessive loss

of carbon and other interstial materials from the stainless steel. If carbon transport from 316 SS proves to be excessive, use of stabilized steels may be necessary. Carbon and nitrogen transfer from stainless steel to Nb-1Zr in potassium at 760°C were reduced or eliminated when 321 SS, containing titanium was substituted for non-stabilized 316 SS.[29] Stabilized alloys also have been effective in controlling carbon transport in liquid sodium systems.[26]

Lithium Purity

Lithium purity is an important consideration in defining the corrosion of materials exposed to a lithium coolant. Impurities in lithium may be grouped into three classes:[30]

1. foreign alkali or alkaline earth metals
2. transition and heavy metals
3. nonmetals, principally oxygen, carbon, hydrogen and nitrogen.

Systematic studies of oxygen and nitrogen effects on stainless steel corrosion in lithium were discussed in an earlier section, indicating that nitrogen at a concentration of 1 wt. percent had an adverse effect at 700°C; oxygen at a similar concentration has very little effect. Other evidence points to nitrogen as the more significant impurity, having an adverse effect on stainless steel corrosion. Systematic studies of metallic impurity effects on stainless steel corrosion in lithium are lacking.

Typical analyses of as-produced lithium are summarized in Table VI. Lithium does not appear to become contaminated by contact with anhydrous gases, (O_2, CO_2, N_2) at least to 160°C. At elevated temperatures, lithium reacts readily with nitrogen to form a nitride.[30]

Table VI

Purity of Commercial Lithium[30]

Metal Grade	99.5%[b]	Reactor[a]
Major Impurities (ppm)	ppm	ppm
Li	--	--
Na	150	40
K	70	75
Rb	--	--
Cs	--	--
Total Alkali Metals	220	115
Alkaline Earths	300	10
Other Metals	150	70
Chlorine	70	50
Oxygen	--	--
Nitrogen	100	40
Carbon	--	--
Hydrogen		
American Producers	Foote Mineral Lithium Corp. Maywood Chemical	
Price/lb (1967)	$9-$11	$12.00

Impurity values in ppm by weight.

[a] Expressed impurity levels are maximum values.

[b] Typical analyses.

Table VII

Influence of Purification Techniques on Lithium Purity

IDENTITY	ppm N	ppm O	ppm C	Ag	Al	B	Be	Ca	Cb	Co	Cr	Cu	Fe	Mg	Mn	Mo	Na	Ni	Pb	Si	Sn	Ti	V	Zr
LITHIUM AS-RECEIVED	835	130	149	<5	<5	--	<5	135	<25	<5	<5	<5	<5	5	<5	<5	55	<5	<25	5	<25	<5	<25	<5
LITHIUM AS RECEIVED AFTER FILTRATION	791	155	90	<5	<5	--	<5	55	<25	<5	<5	<5	<5	5	<5	<5	135	<5	<25	5	<25	<5	<25	<5
LITHIUM AFTER HOT TRAPPING 280 HOURS AT 1500°F	<10	--	25	<5	<5	<55	<5	5	<25	<5	<5	55	5	5	<25	<5	55	5	<25	5	<25	5	<25	<25

Effects of successive purification steps on a given batch of lithium are summarized in Table VII. The as-received impurity content in lithium from a commercial source is shown in the upper analysis. Comparing the as-received analysis in Table VII with Table VI, nitrogen is substantially higher in Table VI; as-received metallic impurities are realtively low in Table VI; oxygen and carbon (not specified in Table VI) are 130 and 149 ppm respectively in the as-received lithium.

Filtering (single-pass) at 205°C through a 5-um sintered Type 316 SS filter had little beneficial effect on impurity levels. However, heating in a titanium-lived zirconium-gettered hot trap at 815°C for 280 hours sharply reduced nitrogen, oxygen, carbon and calcium. The area of the zirconium getter was 6.5 cm^2 per 3.4g of lithium. The zirconium surface area which would be required to clean up 8×10^5kg Li is ~$2 \times 10^6 cm^2$. Assuming a foil thickness of 0.01 cm, the zirconium getter weight in the primary system (LCS, in Figure 1) would be ~10^5kg; while this may not be the optimum amount of zirconium for a large system, it probably is of the right order of magnitude. The amount of getter required for the secondary lithium system would be nearly an order of magnitude less than the primary system requirement. The relatively high getter cost opts for careful pre-purification of lithium and for system design and operation to minimize impurity in-leakage. The fabricated cost of zirconium foil in 1973 is ~$45 per kg. On this basis, the cost of the getter for the primary system would be ~$45 $\times 10^6$, in 1973 dollars. Based on published data,[32] the 0.01-cm foil thickness appears to be marginal and thicker foild may be necessary

depending on the required gettering capacity.

The example cited above (Ref. 31) indicated that zirconium gettered oxygen from lithium to undetectable concentrations, despite indications from thermodynamic data at 870°C that Li_2O is slightly more stable[33] (-105 kcal/g atom O for Zr; -106 kcal/g atom O for Li_2O). Data in Table A-III indicate that between 25 and 625°C the equilibria also slightly favor stability of Li_2O. It is possible that certain impurities in the system altered the thermodynamic relationships or that the thermodynamic data are in error. However, it seems more likely that the thermodynamics of the oxides do not accurately state the energetics of a system where oxygen is dissolving rapidly into the base metal, as it would be expected to do for the case of zirconium at the hot trap temperature (815°C).

Yttrium has been recommended as a hot trap material for lithium systems, because the thermodynamics slightly favor Y_2O_3 formation over Li_2O formation.[33] From the above discussion, it is not clear that yttrium has an advantage over zirconium under actual system operation. Current economics strongly favor zirconium for the hot trap getter.

A major consideration in the design operation of the hot trap is to minimize tritium accumulation in the getter. This essentially rules out steady state hot trap operation with yttrium or zirconium getters because both are strong hydride-formers. However, a sequenced hot trap/tritium extraction bed operation offers a possible prospect for system operation. The entire lithium purification sequence would be as follows:

a) Careful purification of the lithium before charging into the fusion reactor, probably involving filtration, vacuum distillation and possibly hot trapping and special treatments to reduce specific metal impurities.

b) Final purification with the lithium cleanup system;

c) Sequencing of the lithium cleanup and tritium extraction systems; this would occur by allowing the tritium concentration in the lithium blanket to build up to some maximum concentration, dictated by allowable tritium permeation rates through the heat exchanger. This part of the sequence would occur with the extraction and clean-up systems valved out. When the maximum allowable tritium concentration is reached, the extraction system is valved in until the tritium concentration has been reduced to a minimum practicable concentration. The tritium extraction system then would be valved out and the tritium would be removed from the metal getter bed by a high-temperature outgas. The optimum time to valve in the lithium cleanup system would be immediately after the tritium extraction step, when the tritium concentration in the blanket is at a minimum. The lithium cleanup system would be used only as required to maintain acceptable impurity concentrations. On present knowledge, nitrogen appears to be the critical impurity from the standpoint of minimizing stainless steel corrosion. In a previous discussion, the high nitrogen solubility in

lithium was indicated. This makes cold trapping relatively ineffective for nitrogen removal and suggests that a cold trap probably would be unnecessary in the lithium systems.

In sodium, the minimum effective temperature for zirconium hot trap operation was ~550°C.[32] If a similar relationship holds for lithium, it may be necessary to furnish auxiliary heat for reduction of impurities at the beginning of a plant cycle.

Corrosion in Auxiliary Systems

Lithium Cleanup System

Zirconium has functioned successfully as a getter material in a lithium system operating at 816°C.[31] Experience with zirconium getters in sodium systems indicated that the minimum effective temperature is ~540°C.[32]

Zirconium corrosion in high purity lithium was reported as nil after the following exposures: 1070 hours at 816 to 871°C; 400 hours at 1000°C.[24] In general, the corrosion behavior of zirconium in lithium getter applications appears to be satisfactory. Specific data are needed to indicate effects of specific impurities, e.g. carbon and nitrogen on the long-term corrosion and embrittlement of the thin foils in lithium.

Tritium Extraction System

Relatively little is known about yttrium corrosion in lithium at UWMAK-1 temperatures. In the temperature range 1041-1150°C, yttrium was used as a getter in a lithium system.[34] After what appears to have been a 30 hour exposure, the lithium had dissolved 5 wt.%

yttrium; the yttrium corrosion was substantial but not catastrophic. Yttrium forms an oxide slightly more stable in Li_2O at 500°C (Appendix, Table A-III) and is used to getter oxygen from lithium.[33] While this may suppress yttrium dissolution, it also may inhibit tritium extraction and eventually will lead to oxygen saturation of the yttrium. The yttrium carbide also is more stable than lithium carbide and carbides of the major stainless steel components except chromium. Some carbon transport to yttrium therefore may occur. The effect of carbon, nitrogen and oxygen transfer on yttrium corrosion and kinetics of tritium absorption will need to be invesitgated.

Helium Circuit for Cooling the Shield

The helium coolant for the UWMAK-1 shield will be contained in a stainless steel circuit. Preliminary design calculations indicate that the system temperature probabably will not exceed 200°C. The principal impurities in helium are H_2O, air, CO, CO_2, H_2, N_2 and CH_4. The total impurity in the helium can be controlled to about one ppm by volume.[35] Corrosion of stainless steel in helium has not caused problems of metal penetration even at temperatures in the range of 600-930°C.[36] However, sone oxide spallation has occurred at the higher temperatures. At 416°C, 316 SS had a weight loss of 5 mg/dm^2 (~0.06 um) after 1000 hours. Based on the above evidence, it is safe-to assume that corrosion will not be a problem in the shield cooling circuit.

On the contrary, De Van has indicated concern regarding corrosion of niobium in high-purity helium.[16] Other work indicates that substantial corrosion and oxygen solution can occur in niobium at

1000-1200°C in helium having impurity concentrations of ~1 vpm.[35] The basic questions are[a] whether the relative large niobium surface area can getter the impurities initially in the niobium without reaching damaging concentrations of impurities, and[b] whether in-leakage can be controlled to tolerable levels.

Heat Exchanger Corrosion

The lithium-steam interface is a critical area in the context of corrosion control. Stress corrosion cracking failures of steam generators have occurred in nuclear systems.[37] The prospects of lithium-steam reactions and of tritium release to the steam system will require that a highly-reliable steam generator material is available when the first system is built. The design material for the steam generator in this study is 304L stainless steel; tritium diffusion rates are lower for 304 than for 316 SS,[1] and 304 SS is reported to have better metallurgical stability than 316 SS.[2] However, eventual selection of a material with higher resistance to stress corrosion cracking is likely.

Considerable evaluation preceded the selection of Incoloy-800 as the steam generator material for the Westinghouse LMFBR demonstration plant.[2] However, the evidence that nickel-base alloys have relatively poor corrosion resistance in lithium[3] suggests caution in specifying Incoloy or other nickel-base alloys for lithium systems without a comprehensive evaluation.

The trend in liquid metal systems for corrosion to occur at

high-temperature locations and deposition to occur at low-temperature locations will have a strong bearing on steam generator corrosion performance in a lithium-cooled CTR. Experience with steam generators in sodium systems has confirmed minimal corrosion and substantial deposition.[2] However, some selective removal of alloy agents and interstitial impurities has occurred, even at cold-leg locations. Selection of a material which is susceptible to chemical cleaning of fouled heat transfer surfaces probably would be a major consideration in a lithium-cooled stainless steel circuit.

Steam-side corrosion resistance of austenitic stainless steels and nickel-base alloys has proved satisfactory in steam generator applications, from the standpoint of metal penetration. With regard to stress corrosion cracking, not even the nickel-base alloys are immune.[2] Therefore, for the high-integrity need in a lithium-cooled CTR, development of materials with improved stress corrosion resistance and concomitant compatibility with lithium is a major need.

Corrosion Product Transport

Corrosion products generated at one location in a flowing circuit typically are transported and deposited at other locations. This process has caused some problems in water reactors.[38,39] Potential corrosion product problems and associated solutions are being evaluated in LMFBR technology studies, including identification of the types and amounts of mobile corrosion products which are generated[14,28,40-42]; where they deposit; the consequences of the deposits and their associated radioactivity on plant performance;

methods to control and remove the deposits which develop in liquid metal circuits.

Corrosion product deposits up to 0.25 mm thick developed in a stainless steel circuit exposed to sodium for 10,000 hours at 720°C (hot leg) and 550°C (cold leg).[40] The amount and composition of deposits varies with location in the circuit. Deposition varied as a function of temperature, coolant velocity, turbulence level, and operating time. Temperature differences as small as ~30°C promoted deposition. Maximum deposition occurred at the lowest temperatures in the circuit. The deposition rates generally decreased with exposure time, tending to reach a steady-state rates of 0.1 to 0.2 mg/cm^2 hr after a few thousand hours.

In fusion reactor systems relying on lithium of molten salts for heat transfer, corrosion product transport considerations may have a significant bearing on materials selection and plant design. The four essential factors considered here are: corrosion product generation, transport, deposition and removal.

Corrosion product generation in CTR's is amplified by the relatively large areas in contact with the primary coolant. The system parameters which apply to the Wisconsin Toroidal Fusion Reactor (UWMAK-I)appear in Table II. The primary circuit area is $6 \times 10^4 m^2$; by comparison, the area of the Fast Flux Test Facility (FFTF) primary circuit is $\sim 1 \times 10^3 m^2$.[14]

Accurate assessment of corrosion phenomena in lithium-cooled CTR's is compromised by the relatively small amount of pertinent data. The UWMAK-1 lithium inlet and outlet temperatures are

~300 and 500°C. Corresponding stainless steel corrosion rates are reported to be 0.01 and 1 mg/cm^{2}mo based on the data of Gill, et al in exposures to flowing lithium (15-85 cm/sec).[5] These corrosion rates, extended to an annual basis, indicate that approximately 2500 kg/y of corrosion product would be released to the primary circuit. In addition to the thermal corrosion cited above, a potential substantial contribution from radiation sputtering on the inside surface of the first wall was identified in an earlier section, amounting to about ten percent of the thermal value (~250 kg/y). Further increases in corrosion rate also may occur if sputtering removes a rate-controlling layer from the stainless steel surface.

While the accuracy of the calculated rates of corrosion product release are in question, the magnitudes focus on the importance of considering corrosion product generation and transport in future experiments and eventually in plant design and materials selection if the order of magnitude is correct.

The corrosion of 316 SS in lithium at 500-600°C does not release the individual constituents in the stoichiometry shown in Table I. Nickel is reported to be the principal element transferred; chromium, maganese, silicon, and carbon were detectable in the stainless steel corrosion product deposits.[5,7] Selective leaching of nickel results in development of a ferrite phase on the corroding stainless steel surface. The corrosion rate reportedly is controlled by

solid-phase diffusion through the ferrite layer in the temperature range of 510-610°C.[5,8] Corrosion data for other CTR candidate materials (alloys of Mo, Nb, and V) suggest that corrosion product transport rates from thermal corrosion may be orders of magnitude lower than those calculated for stainless steel, even at higher operating temperatures projected for CTR's constructed from the refractory metals. The corrosion rates generally are reported as "nil" or "slight". Quantitative corrosion rate data for a Nb-1Zr alloy in flowing lithium at 1200°C indicate that the corrosion product transport rate would be ~5 kg/y[9] in a system having the area shown in Table II. The 5 kg would include principally N, C and Zr. Very little Nb was found in the transferred deposits.

On the other hand, sputtering may contribute to sizable mass transport for the refractory metals, paralleling the earlier calculation for stainless steel. Assuming a niobium sputtering rate perhaps a factor of two lower[21] than the number used in the stainless steel calculation, sputtering from the first wall would propel ~125 kg/y into the circulating lithium.

Corrosion rates cited earlier for stainless steel in flibe are on the order of 25 um/y at 650-680°C.[10] The temperature range is neat the operating temperature of a helium-cooled CTR having a molten salt blanket.[43] Since the flibe is not the heat transfer medium, corrosion product transport and deposition will be less severe than in lithium-cooled stainless steel plants. However, circulation of the flibe to the tritium extraction system almost certainly would result in radiation problems and possibly fouling

and plugging, in view of the relatively high stainless steel corrosion rates.

Mechanisms of corrosion product transport include dissimilar-metal mass transfer and temperature gradient mass transfer. Both types will occur in the UWMAK-1 circuits. Dissimilar metal transfer can occur between stainless steel, zirconium getter beds, and the yttrium metal in the tritium extraction beds. Temperature gradient mass transfer will occur by dissolution of stainless steel in the high-temperature regions and deposition in the low-temperature regions.

Corrosion products will be carried to all parts of a lithium-cooled primary circuit in solution and also possibly as particulates; with maximum deposition occurring in the heat exchanger and tritium extraction system. Potential problems due to corrosion product deposition in the primary CTR unit include: fouling of heat transfer surfaces; plugging of heat exchanger tubes, valves and instrument sensor lines; fouling of tritium extraction surfaces; development of high radiation levels in reactor maintenance areas. The radioactivity content of 2500 kg of stainless steel corrosion product is estimated to be 4×10^6 curies. Radiation levels in an FFTF heat transport system cell are estimated to be 1 to 15 Rad/hr,[3] based on a stainless steel corrosion product inventory which appears to be approximately three orders of magnitude below the estimated CTR inventory, portending that relatively high radiation fields would develop near out-of-reactor regions of a stainless steel CTR circuit. Based on half life considerations, stainless steel is the least desirable and vanadium appears to be

the most desirable for rapid decay of activity in reactor maintenance areas.[8]

Stainless steel is the only CTR candidate material with a well-developed industry, opting for its consideration as a construction material in first-generation plants. If this incentive persists as the time to build the first plant approaches, a major effort will be needed to determine corrosion and corrosion product transport rates under prototypical CTR conditions. Extraction of corrosion products from the primary system almost certainly would be required if the estimated transport rate is accurate.

Preliminary studies are underway to investigate corrosion product removal from LMFBR systems, either continuously[45] or by dissolution of deposits during plant shutdowns.[42] Possible methods for continuous corrosion product removal include hot trapping, cold trapping and high temperature ion exchange. However, the technology for successfully applying these methods remains to be developed. Proper selection of materials, e.g., minimizing cobalt in the primary loop, can assist in control of radiation buildup in maintenance areas. Early studies of decontamination techniques for LMFBR systems are underway,[42] but are in early stages. Successful operation of lithium-cooled stainless steel CTRs almost certainly would require technology development for corrosion product control paralleling that now underway for LMFBR systems.

References

1. R. W. Webb, Permeation of Hydrogen Through Metals, NAA-SR-10462, July 1965.

2. W. E. Ray, S. L. Schrock, S. A. Shiels and K. C. Thomas, "Selection of Steam Generator Tubing Material for the Westinghouse LMFBR Demonstration Plant," Nucl. Tech. 11 222 (1971).

3. R. N. Lyon (Ed.), Liquid Metals Handbook, Report NAVEXOS-P-733 (Rev.), Superintendent of Documents, U. S. Government Printing Office, p. 158ff, June 1952.

4. M. S. Goikhman, A. M. Datisishin, I. G. Shtykalo, V. F. Shatinskii, and M. I. Chaevskii, "Corrosion Failure of 1Cr18Ni9Ti Steel in Liquid Lithium," Soviet Materials Science, 6 491 (1968).

4a. V. V. Popovich, M. S. Goikhman, E. I. Polyakov and M. I. Chaevskii, "The Effects of Lithium on the Mechanical Characteristics of Austenitic Stainless Steels," Soviet Materials Science, 5, 345 (1969).

5. W. N. Gill, R. P. Vanek, R. V. Jelinek and C. S. Grove, Jr., "Mass Transfer in Liquid-Lithium Systems," AIChE Journal 6, 139 (1960).

6. Dai-Kai Sze and W. E. Stewart, Thermal and Mechanical Design Considerations for Lithium-Cooled Tokamak Reactor Blankets, University of Wisconsin Fusion Design Memo No., 41, March 1973.

7. J. H. Strong, E. M. Simons, J. A. DeMastry and J. M. Genco, Compatibility of Liquid and Vapor Alkali Metals with Construction Materials DMIC Report 227, April 1966, p. 89.

8. H. W. Leavenworth and D. P. Gregory, "Mass Transfer of Type 316 Stainless Steel by Liquid Lithium," Corrosion, 18, 43t (1962).

9. J. H. DeVan and C. E. Sessions, "Mass Transfer of Niobium-Base Alloys in Flowing Non-Iso-Thermal Lithium," Nucl. Appl. 3 102 (1967).

10. J. M. Kroger, Alloy Compatibility with LiF-BeF_2 Salts, ORNL-TM-4286, in press.

11. R. E. Seebold, L. S. Birks, and E. J. Brooks, "Selective Removal of Chromium from Type 304 Stainless Steel by Air-Contaminated Lithium," Corrosion, 16, 468t, (1960).

12. E. E. Hoffman, "Liquid Metal Corrosion," Symposium on Corrosion Fundamentals A. de A. Brasumas and E. E. Stausburg, Eds., Univ. of Tenn. Press, p. 65ff, 1956.

13. G. DeVries, "The Corrosion of Metals by Molten Lithium," Corrosion by Liquid Metals, J. E. Draley and J. R. Weeks, Eds. Plenum Press, p. 251ff, 1970.

14. T. J. Kabele, W. F. Brehm and D. R. Marr, "Activated Corrosion Product Radiation Levels in FFTF," Trans. Am. Nucl. Soc. 16, 108 (1973). See also HEDL-TME-72-71 (1972).

15. R. L. Klueh, Effect of Oxygen on the Corrosion of Nb and Ta by Liquid Lithium, ORNL-TM-4069, March 1973.

16. J. H. DeVan, "Compatibility" Fusion Reactor First Wall Materials, L. C. Iannielle, Ed. p. 25-29, April 1972.

17. W. E. Berry, Corrosion in Nuclear Applications Wiley, New York, p. 293.

18. W. E. Berry, loc. cit. p. 256.

19. J. N. Anno and J. A. Walowit, "Analysis of Corrosion of Stainless Steel in a Sodium and High Radiation Environment," Nucl. Tech. 10 67, (1971).

20. W. E. Berry, Loc. cit., p. 252-3.

21. G. L. Kulcinski, Personal Communication, University of Wisconsin, July 30, 1973.

22. A. B. Johnson, Jr., "Aqueous Corrosion and Hydriding of Zirconium Alloys in Nuclear Reactors Environments," Proceedings of the Fourth International Congress on Metallic Corrosion, Sept. 7-14, 1969 Amsterdam, p. 168. National Association of Corrosion Engineers, 1972.

23. R. E. Cleary, S. S. Polecherman and J. E. Corliss, "Solubility of Refractory Metals in Lithium and Potassium," TTM-850, November 1965. See Also, W. E. Berry, Corrosion in Nuclear Applications Wiley & Sons, New York, 1971, p. 291.

24. E. J. Cairns, F. A. Cafasso and V. A. Maroni, A Review of the Chemical, Physical and Thermal Properties of Lithium that are Related to its Use in Fusion Reactors, The Chemistry of Fusion Technology, D. E. Gruen, Ed., Plenum Press, New York, 1972, p. 116; 129 ff.

25. J. R. DiStefano and A. P. Litman, "Effects of Impurities in Some Refractory Metal - Alkali Metal Systems," Corrosion, 20, 392t (1964).

26. J. R. Weeks and H. S. Isaacs, "A General Model for the Corrosion of Steels in High Velocity Sodium," Chemical Aspects of Corrosion and Mass Transfer in Liquid Sodium, S. A. Jansson, Ed., Metallurg Soc. AIME. p. 207 (1972).

27. J. O. Cowles and A. D. Posternak, Lithium Properties Related to Use as a Nuclear Reactor Coolant, UCRL-50647, April 1969.

28. G. D. Collins, Summary Report - Sodium Mass Transfer Program - Effects of Sodium Exposure on the Corrosion and Strength of Stainless Steels, GEAP-10394, August 1971.

29. J. W. Semmel, Jr., L. B. Engel, Jr., R. G. Frank and R. W. Harrison, "Carbon Mass Transfer in Multimetallic Systems Containing Potassium," Alkali Metal Coolants Proceedings of Symposium, Vienna, Nov. 28 - Dec. 2, 1966, International Atomic Energy Agency, Vienna, 1967 p. 181ff.

30. J. E. Maustoller, F. Topper, S. J. Rodgers, Alkali Metal Handling and Systems Operating Techniques, AEC Monograph, Gorden and Breack, New York, 1967, p. 8-34.

31. R. W. Harrison, "The Effect of Welding Atmosphere Purity on the Lithium Corrosion Resistance of Refractory Alloys" Corrosion by Liquid Metals, J. E. Draley and J. R. Weeks, Plenum Press, New York, 1970, p. 223ff.

32. F. A. Kozlov and E. K. Kuznetsov, "The Use of Hot Traps for Removing Oxygen from Sodium," Liquid Metals, P. L. Kinllov, et al, Ed., NASA-TT-F-522, May 1969, p. 340.

33. J. E. Manstoller, et al, loc. cit., p. 61-64.

34. W. M. Phillips, "Some Alkali Metal Corrosion Effects in a Rankine Cycle Test Loop," Corrosion by Liquid Metals, J. E. Draley and J. R. Weeks, Eds., Plenum Press, 1970, p. 214.

35. L. A. Charlot and R. E. Westerman, High Temperature Corrosion of Candidate ATE Structural Materials, BNWL-100, September 1965.

36. W. E. Berry, loc. cit., p. 394.

37. S. H. Bush and R. L. Dillon, "Stress Corrosion in Nuclear Systems" paper for presentation at the International Conference on Stress Corrosion Cracking and Hydrogen Embrittlement of Iron Base Alloys, Firminy, France, June 1973.

38. G. J. Walke, R. W. Sinderman, C. E. Axtell, "The Effects of Failed Fuel on the Operation of a Commercial BWR Plant," Trans. Am. Nucl. Soc. 13, 165 (1970).

39. D. H. Charlesworth, "Water Reactor Plant Contamination and Decontamination Requirements - A Survey," Proceed. of Am. Power Conf. 33, 749 (1971).

40. W. E. Ray, R. L. Miller, S. L. Schrock, and G. A. Whitlow, "Structure of Sodium Corrosion Deposits and Their Effect on Heat Transfer Coefficients," Nucl. Tech. 16 249 (1972).

41.